JACS
JOURNAL OF THE AMERICAN CHEMICAL SOCIETY
Communication
pubs.acs.org/JACS

Growth of p-Type Hematite by Atomic Layer Deposition and Its Utilization for Improved Solar Water Splitting

Yongjing Lin,‡ Yang Xu,‡ Matthew T. Mayer, Zachary I. Simpson, Gregory McMahon, Sa Zhou, and Dunwei Wang*

Department of Chemistry, Merkert Chemistry Center, Boston College, 2609 Beacon Street, Chestnut Hill, Massachusetts 02467, United States

Supporting Information

ABSTRACT: Mg-doped hematite (α-Fe_2O_3) was synthesized by atomic layer deposition (ALD). The resulting material was identified as p-type with a hole concentration of ca. 1.7×10^{15} cm^{-3}. When grown on n-type hematite, the p-type layer was found to create a built-in field that could be used to assist photoelectrochemical water splitting reactions. A nominal 200 mV turn-on voltage shift toward the cathodic direction was measured, which is comparable to what has been measured using water oxidation catalysts. This result suggests that it is possible to achieve desired energetics for solar water splitting directly on metal oxides through advanced material preparations. Similar approaches may be used to mitigate problems caused by energy mismatch between water redox potentials and the band edges of hematite and many other low-cost metal oxides, enabling practical solar water splitting as a means for solar energy storage.

Solar water splitting harvests the energy in sunlight and stores it in chemical forms, promising a solution to the challenge associated with the diurnal nature of solar energy.[1] For the technology to be economically competitive, we need nontoxic materials that are earth abundant and capable of performing the reactions at high efficiencies.[2] Among examined candidates, hematite (α-Fe_2O_3) stands out for its suitable band gap, stability, and abundance.[3] Notwithstanding its appeals, hematite presents significant challenges as well. For example, its hole diffusion distance is on the order of a few nanometers (nm), greatly limiting the efficiency of charge collection.[4] To address this issue, researchers have proposed and demonstrated methods such as doping or introducing additional charge transport components.[5] Slow charge transfer kinetics at the solid−electrolyte interface is another challenge one needs to overcome for high efficiencies. Catalysts of various natures have been shown as potential solutions to this issue if deposited properly on the surface of hematite.[6] Yet, a fundamental challenge of hematite, the significant mismatch between the band edge positions and the water reduction and oxidation potentials, has received little attention.[7] This mismatch will have at least two important implications. First, with the conduction band edge more positive than the potential at which H_2O is reduced to H_2, complete water splitting cannot be achieved without applied biases. Second, the valence band edge is too positive to permit the measurement of high photovoltage for the oxidation of H_2O to O_2, limiting the practical power conversion efficiencies.

In principle, the energy mismatch problem can be solved by forming junctions within the semiconductors.[8] For instance, Turner et al. have measured record-high solar water splitting efficiency on devices made of GaAs and $GaInP_2$ junctions;[8b] more recently, Nocera et al. achieved complete water splitting using triple junctions of amorphous Si.[8c] Being able to apply similar approaches to hematite or other low-cost semiconducting metal oxides should have significant value because it has the potential to solve a key challenge of these otherwise attractive materials. Energy diagrams of such a system are schematically illustrated in Figure 1a,b on a simplistic planar geometry (with illumination). For a system in vacuum, one can measure a photovoltage up to V_{ph} when an n−p junction exists. In the absence of p-type coating, no photovoltage is expected from n-type hematite. When in contact with H_2O, however, a significant surface potential due to surface adsorption can build up on the surface of n-type hematite. This potential allows for the measurement of a photovoltage of V_{ph}'. As such, for hematite in contact with H_2O, the difference between V_{ph} and V_{ph}' ($\Delta V_{ph} = V_{ph} - V_{ph}'$) would be what one gains by forming a buried n−p junction. Here, we show that even without optimization, this difference is substantial, on the order of hundreds of millivolts (mV), comparable to the effect exhibited by catalysts.

Although p-type hematite has been studied previously,[9] a synthesis to enable the construction of high quality n−p junctions was absent in the literature. Our first task was therefore to correct this deficiency. We sought to realize this goal using atomic layer deposition (ALD) for two reasons. First, ALD is known to permit the growth of hetero- or homojunctions with low defect densities.[10] Second, the excellent conformability offered by ALD makes it possible to form nanostructures of hematite, which can be further exploited for charge transport management, as has been recently demonstrated by us.[11] We used bis(ethylcyclopentadienyl) magnesium as the Mg precursor,[12] and the precursor for Fe was iron *tert*-butoxide.[13] For a typical growth, the Mg precursor was introduced once every 5 cycles of repeated pulses of Fe precursors and H_2O. A 20 nm thick film was produced by 400 cycles of deposition (measured by Fe precursor pulses), resulting in a Mg concentration of ca. 3% (Figure 1c). Other

Received: January 23, 2012
Published: March 7, 2012

   dx.doi.org/10.1021/ja300319g | *J. Am. Chem. Soc.* 2012, 134, 5508−5511

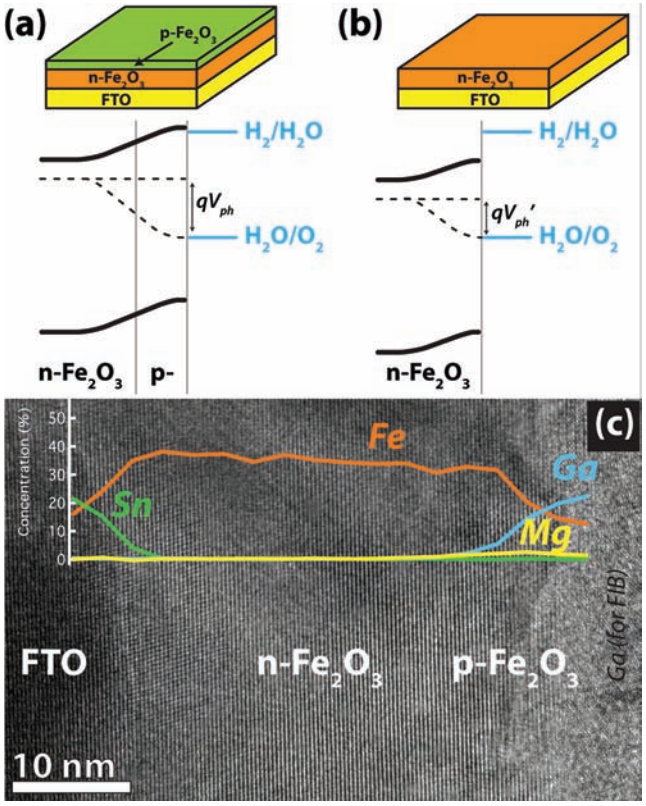

Figure 1. Energy band diagrams and microstructures of hematite with a p-type coating. (a) The introduction of a p-type layer creates a built-in field that does not depend on surface adsorptions, allowing for the measurement of a more substantial photovoltage (V_{ph}). The device structure is schematically illustrated on top. (b) In comparison, although a built-in field can also be achieved on n-type hematite, its depth and magnitude are sensitive to the nature of the electrolyte. (c) Cross-sectional transmission electron micrograph (TEM) of the n–p junction. Inset: line-scan of energy dispersive spectra (EDS) of various elements across the film. See SI for an overall EDS survey scan on p-type only Fe_2O_3.

variants of parameters have been studied as well, and the details are provided in the Supporting Information (SI). Importantly, the introduction of Mg to the growth did not alter the crystal structure or morphology of ALD-grown Fe_2O_3 (Figure S1 in SI), ruling out possibilities that these factors may play a role in the photoelectrochemical effects to be discussed below.

We performed a series of experiments, including photoelectrochemical (PEC) characterizations and electrochemical impedance measurements, to verify that the Mg-doped hematite was indeed p-type. The optical absorption was characteristic of hematite without intentional doping (inherently n-type), proving that the inclusion of Mg did not change the optical properties of hematite measurably (Figure S3 in SI). A cathodic current was measured when Mg-doped hematite was measured under illumination (Figure 2a). In the absence of electron scavengers, the cathodic current was due to O_2 reduction. By contrast, cathodic currents were not observed under similar measurement conditions by n-type Fe_2O_3. The most direct evidence that the film is p-type comes from the negative slope obtained when the capacitance was plotted against the applied potentials (Mott–Schottky plot, Figure 2b), from which a hole concentration of 1.7×10^{15} cm^{-3} was calculated. Extrapolation of the Mott–Schottky plot also yielded a flat band potential (V_{fb}) of 1.24 V versus RHE

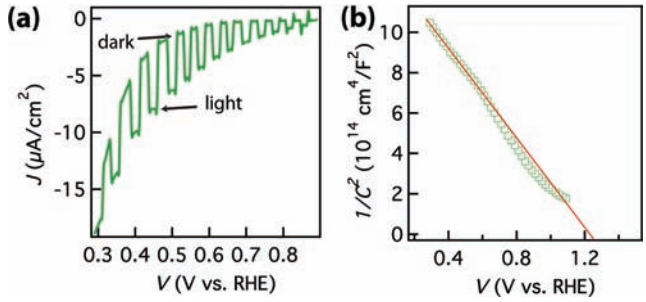

Figure 2. Characterizations of Mg-doped hematite (20 nm in thickness). (a) A cathodic current was measured under illumination. The measurements were carried out in 1 M KOH solution; (b) Mott–Schottky plot (in 1 M KOH).

(reversible hydrogen electrode; all potentials henceforward are relative to RHE unless noted), which is significantly more positive than that of nonintentionally doped hematite synthesized by ALD in our lab (0.67 V),[11d] indicating a considerable shift of the Fermi level toward the valence band edge.

Next we sought to form n–p junctions by directly growing Mg-doped Fe_2O_3 (5 nm) on iron oxide without intentional doping (20 nm), which is inherently n-type due to O vacancies. Microstructure studies proved that the resulting film was of a polycrystalline nature. It is important to note that no grain boundary was observed between p- and n-type Fe_2O_3 (Figure 1c). We therefore conclude that the growth of p-type Fe_2O_3 does not introduce additional structural defects. PEC measurements revealed a stark difference in the turn-on characteristics between Fe_2O_3 with and without the p-type coating, as shown in Figure 3a. While no significant photocurrent was detected

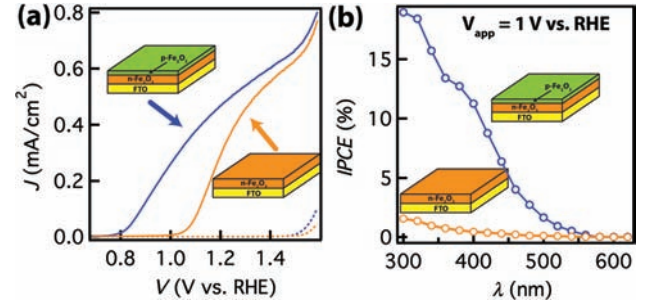

Figure 3. Photoelectrochemical characterizations of n-type Fe_2O_3 with and without p-type coating (total thickness: 25 nm). (a) A significant reduction of the turn-on voltage was observed on the sample with p-Fe_2O_3. Data measured under 1 Sun conditions (100 mW/cm^2, AM 1.5 G). Dark currents shown in dashed lines. (b) IPCE characteristics of these samples at 1 V.

below 1 V for n-type Fe_2O_3, with Mg–Fe_2O_3 coating it exhibited a turn-on voltage of ca. 0.8 V, representing a −0.2 V shift. The incident photon to charge conversion efficiencies (IPCE) were also recorded at 1 V applied potential to verify this effect (Figure 3b). The reduction of required bias is significant because it is comparable to what has been achieved by improving charge transfer through additions of catalysts.[6b,d]

Several other competing mechanisms might be used to explain the observed difference. For instance, Gratzel and Sivula et al. have recently shown that deposition of oxides on the surface of Fe_2O_3 could introduce a "passivation" effect.[14] We ruled out this possibility by control experiments where the

dx.doi.org/10.1021/ja300319g | J. Am. Chem. Soc. 2012, 134, 5508–5511

surface of Fe_2O_3 was coated with a thin layer of MgO. The resulting material showed poorer PEC performance than bare Fe_2O_3 (Figure S5). Another factor to consider was the total film thickness (20 nm for bare Fe_2O_3 and 25 nm for that with Mg-doped Fe_2O_3), which may influence PEC behavior. To examine this possibility, we grew an additional 5 nm n-Fe_2O_3 on top of a 20 nm thick pregrown n-type sample, producing a total thickness of 25 nm. The growth procedure was identical to the two-step growth of n−p junction samples. Different from samples with n−p junctions, however, the 25 nm-thick film did not exhibit the cathodic shift (Figure S6). Lastly, one can envision that if the sequence of the p- and n-Fe_2O_3 layers was reversed, that is, coating n-type Fe_2O_3 on top of the p-type one, a trap would be created by the p-type layer to compete with surface H_2O in receiving photogenerated holes. Indeed, this hypothesis was in agreement with our experimental observations, wherein anodic photocurrent was greatly reduced (Figure S7). Taken as a whole, this evidence supports that the mechanism we hypothesized in Figure 1 is reasonable and explains the measured turn-on voltage shift.

Because of the thinness of films studied here, the band diagrams presented in Figure 1 may need refinements for more quantitative discussions. However, any modifications will unlikely change the consideration about improved solar water splitting on a fundamental level. In essence, the concept we proved was that the existence of the n−p junction within Fe_2O_3 leads to changes of photocurrents toward the cathodic direction. At least two experiments can be used to help visualize the existence of this junction. The first one is based on the assumption that the capacitance of the junction can be measured by electrochemical impedance spectroscopy (EIS). In the Nyquist plots shown in Figure 4a, a semicircle was obtained

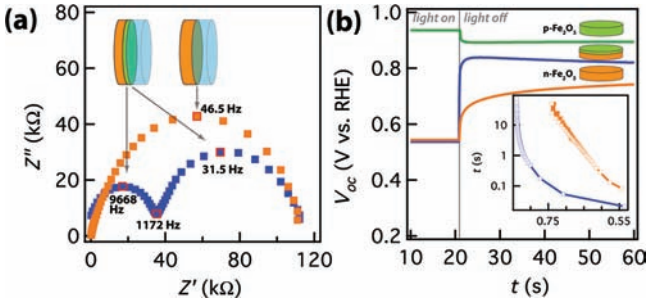

Figure 4. Visualization of the n−p junction within Fe_2O_3. (a) A clear difference is visible between the Nyquist plots of n- (brown) and n−p (blue) Fe_2O_3 (measured at 1.7 V vs RHE). To assist viewing, the assignments of the semicircles are illustrated by schematics of device structures (H_2O shown in translucent blue). Several key data points are highlighted, with the corresponding frequencies labeled. (b) Open circuit voltage decay for p-, n-, and n−p Fe_2O_3. Inset: time constant of the decay plotted in semilogarithm scale. Label for *x*-axis: *V* vs RHE.

on n-Fe_2O_3. We attributed its origin to the depletion of Fe_2O_3 due to the contact with the electrolyte but not the Helmholtz double layer because of the frequency range (peaking at ca. 46 Hz) within which it was measured. In contrast, two semicircles were observed on Fe_2O_3 with the n−p junction, one in the frequency range (peaking at ca. 31 Hz) similar to that of n-Fe_2O_3, the other in the high frequency range (peaking at ca. 10 kHz), which we attributed to the n−p junction. Because the measurements were performed in dark, the system impedance was dominated by charge transfer at potentials below 1.6 V, and that was why we obtained the plots in Figure 4a at 1.7 V.

The second technique to help us see the existence of the built-in field relies on how the field affects charge behaviors. Under illumination, this field facilitates charge separation; conversely, under transient conditions when the illumination is stopped, the junction should be a preferable site for photogenerated electrons and holes to recombine. As such, one would expect accelerated open circuit voltage (V_{oc}) decay when illumination is removed. This was indeed observed. Shown in Figure 4b are the comparison between p-, n-, and n−p Fe_2O_3. That a negative change of the open circuit voltage was observed upon removing illumination from Mg-doped Fe_2O_3 further supports that we have successfully obtained p-type Fe_2O_3. Also note that the nature of the n-p Fe_2O_3 behavior is similar to n-Fe_2O_3 for two reasons: the film is predominantly n-type with a thin p-type coating, and the measurement conditions favor hole transfer to the solution. Using the methodology developed by Bisquert et al.,[15] we see in the inset the open circuit voltage decay for n−p Fe_2O_3 is faster than n-Fe_2O_3 by at least an order of magnitude. The fast decay kinetics is indicative of insignificant charge trapping when illuminated and, hence, effective charge separation under water splitting conditions. We also emphasize that the lower bound of the time constant (~100 ms) is limited by our apparatus. The process likely takes place on a faster time scale.

Building internal fields by the introduction of homojunctions buried in a semiconductor through doping control has been a classical approach for the construction of electronic devices and solar cells. However, this concept has not been previously demonstrated on semiconducting metal oxides consisting of earth abundant elements such as hematite. An important reason for this deficiency is the lack of growth control. The advantage as illustrated in Figure 1 will diminish if the synthesis method is prone to produce defects between the p- and n-type layers. We have shown that ALD is a technique that has the potential to correct the deficiency. Through growth control, we successfully produced n−p junctions within Fe_2O_3. Importantly, no obvious structural defects between p- and n-type Fe_2O_3 were observed. As a result, a ca. 200 mV turn-on voltage shift toward the cathodic direction was observed. The magnitude is comparable to what has been reported by using water oxidation catalysts, although the latter functions through a fundamentally different mechanism of overpotential reduction.

■ ASSOCIATED CONTENT

Supporting Information

Synthesis of Fe_2O_3 and Mg-doped Fe_2O_3 by ALD, optical and photoelectrochemical characterization of Mg-doped Fe_2O_3, photoelectrochemical measurement of control samples. This material is available free of charge via the Internet at http://pubs.acs.org.

■ AUTHOR INFORMATION

Corresponding Author

dunwei.wang@bc.edu

Author Contributions

‡These authors contributed equally.

Notes

The authors declare no competing financial interest.

■ ACKNOWLEDGMENTS

The work is funded by an NSF CAREER award (DMR1055762). The acquisition of FIB used for this work

was supported by NSF (DMR 0821471). The XPS measurement was performed at Center for Nanoscale Systems, which is a member of the National Nanotechnology Infrastructure Network (NNIN), supported by NSF (ECS-0335765). We thank L. Qin and J. Gao for helping synthesize iron *tert*-butoxide. We also thank G. Yuan, J. Bisquert, S. Boettcher, and C. K. Tsung for their insightful suggestions, and D. Wang for his assistance with TEM.

REFERENCES

(1) (a) Bak, T.; Nowotny, J.; Rekas, M.; Sorrell, C. C. *Int. J. Hydrogen Energy* **2002**, *27*, 991. (b) Kudo, A.; Miseki, Y. *Chem. Soc. Rev.* **2009**, *38*, 253. (c) Chen, X.; Shen, S.; Guo, L.; Mao, S. S. *Chem. Rev.* **2010**, *110*, 6503. (d) Lewis, N. S.; Nocera, D. G. *Proc. Natl. Acad. Sci. U.S.A.* **2006**, *103*, 15729. (e) Lin, Y.; Yuan, G.; Liu, R.; Zhou, S.; Sheehan, S. W.; Wang, D. *Chem. Phys. Lett.* **2011**, *507*, 209.

(2) (a) Youngblood, W. J.; Lee, S.-H. A.; Maeda, K.; Mallouk, T. E. *Acc. Chem. Res.* **2009**, *42*, 1966. (b) Osterloh, F. E. *Chem. Mater.* **2007**, *20*, 35. (c) Walter, M. G.; Warren, E. L.; McKone, J. R.; Boettcher, S. W.; Mi, Q.; Santori, E. A.; Lewis, N. S. *Chem. Rev.* **2010**, *110*, 6446.

(3) (a) Sivula, K.; Le Formal, F.; Grätzel, M. *ChemSusChem* **2011**, *4*, 432. (b) Lin, Y.; Yuan, G.; Sheehan, S.; Zhou, S.; Wang, D. *Energy Environ. Sci.* **2011**, *4*, 4862. (c) McDonald, K. J.; Choi, K.-S. *Chem. Mater.* **2011**, *23*, 4863. (d) Gonçalves, R. H.; Lima, B. H. R.; Leite, E. R. *J. Am. Chem. Soc.* **2011**, *133*, 6012. (e) Gao, H.; Liu, C.; Jeong, H. E.; Yang, P. *ACS Nano* **2012**, *6*, 234.

(4) Dareedwards, M. P.; Goodenough, J. B.; Hamnett, A.; Trevellick, P. R. *J. Chem. Soc., Faraday Trans. 1* **1983**, *79*, 2027.

(5) (a) Kay, A.; Cesar, I.; Gratzel, M. *J. Am. Chem. Soc.* **2006**, *128*, 15714. (b) Sivula, K.; Zboril, R.; Le Formal, F.; Robert, R.; Weidenkaff, A.; Tucek, J.; Frydrych, J.; Gratzel, M. *J. Am. Chem. Soc.* **2010**, *132*, 7436. (c) Hu, Y. S.; Kleiman-Shwarsctein, A.; Forman, A. J.; Hazen, D.; Park, J. N.; McFarland, E. W. *Chem. Mater.* **2008**, *20*, 3803. (d) Hahn, N. T.; Mullins, C. B. *Chem. Mater.* **2010**, *22*, 6474. (e) Ling, Y.; Wang, G.; Wheeler, D. A.; Zhang, J. Z.; Li, Y. *Nano Lett.* **2011**, *11*, 2119. (f) Wang, G.; Ling, Y.; Wheeler, D. A.; George, K. E. N.; Horsley, K.; Heske, C.; Zhang, J. Z.; Li, Y. *Nano Lett.* **2011**, *11*, 3503. (g) Lukowski, M. A.; Jin, S. *J. Phys. Chem. C* **2011**, *115*, 12388. (h) Saretni-Yarahmadi, S.; Wijayantha, K. G. U.; Tahir, A. A.; Vaidhyanathan, B. *J. Phys. Chem. C* **2009**, *113*, 4768. (i) Mor, G. K.; Prakasam, H. E.; Varghese, O. K.; Grimes, C. A. *Nano Lett.* **2007**, *7*, 2356. (j) LaTempa, T. J.; Paulose, M.; Grimes, C. A. *J. Phys. Chem. C* **2009**, *113*, 16293.

(6) (a) Zhong, D. K.; Sun, J.; Inumaru, H.; Gamelin, D. R. *J. Am. Chem. Soc.* **2009**, *131*, 6086. (b) Tilley, S. D.; Cornuz, M.; Sivula, K.; Grätzel, M. *Angew. Chem., Int. Ed.* **2010**, *49*, 6405. (c) McDonald, K. J.; Choi, K.-S. *Chem. Mater.* **2011**, *23*, 1686. (d) Zhong, D. K.; Cornuz, M.; Sivula, K.; Gratzel, M.; Gamelin, D. R. *Energy Environ. Sci.* **2011**, *4*, 1759.

(7) Brillet, J.; Cornuz, M.; Formal, F. L.; Yum, J.-H.; Grätzel, M.; Sivula, K. *J. Mater. Res.* **2010**, *25*, 17.

(8) (a) Hwang, Y. J.; Boukai, A.; Yang, P. *Nano Lett.* **2008**, *9*, 410. (b) Khaselev, O.; Turner, J. A. *Science* **1998**, *280*, 425. (c) Reece, S. Y.; Hamel, J. A.; Sung, K.; Jarvi, T. D.; Esswein, A. J.; Pijpers, J. J. H.; Nocera, D. G. *Science* **2011**, *334*, 645. (d) Boettcher, S. W.; Warren, E. L.; Putnam, M. C.; Santori, E. A.; Turner-Evans, D.; Kelzenberg, M. D.; Walter, M. G.; McKone, J. R.; Brunschwig, B. S.; Atwater, H. A.; Lewis, N. S. *J. Am. Chem. Soc.* **2011**, *133*, 1216.

(9) (a) Turner, J. E.; Hendewerk, M.; Parmeter, J.; Neiman, D.; Somorjai, G. A. *J. Electrochem. Soc.* **1984**, *131*, 1777. (b) Ingler; Baltrus, J. P.; Khan, S. U. M. *J. Am. Chem. Soc.* **2004**, *126*, 10238.

(10) Parsons, G. N.; George, S. M.; Knez, M. *MRS Bull.* **2011**, *36*, 865.

(11) (a) Lin, Y.; Zhou, S.; Liu, X.; Sheehan, S.; Wang, D. *J. Am. Chem. Soc.* **2009**, *131*, 2772. (b) Liu, R.; Lin, Y.; Chou, L.-Y.; Sheehan, S. W.; He, W.; Zhang, F.; Hou, H. J. M.; Wang, D. *Angew. Chem., Int. Ed.* **2011**, *50*, 499. (c) Liu, X.; Lin, Y.; Zhou, S.; Sheehan, S.; Wang, D. *Energies* **2010**, *3*, 285. (d) Lin, Y.; Zhou, S.; Sheehan, S. W.; Wang, D. *J. Am. Chem. Soc.* **2011**, *133*, 2398. (e) Klahr, B. M.; Martinson, A. B. F.; Hamann, T. W. *Langmuir* **2011**, *27*, 461. (f) Martinson, A. B. F.; DeVries, M. J.; Libera, J. A.; Christensen, S. T.; Hupp, J. T.; Pellin, M. J.; Elam, J. W. *J. Phys. Chem. C* **2011**, *115*, 4333.

(12) Burton, B. B.; Goldstein, D. N.; George, S. M. *J. Phys. Chem. C* **2009**, *113*, 1939.

(13) Bachmann, J.; Jing; Knez, M.; Barth, S.; Shen, H.; Mathur, S.; Gösele, U.; Nielsch, K. *J. Am. Chem. Soc.* **2007**, *129*, 9554.

(14) (a) Hisatomi, T.; Le Formal, F.; Cornuz, M.; Brillet, J.; Tetreault, N.; Sivula, K.; Gratzel, M. *Energy Environ. Sci.* **2011**, *4*, 2512. (b) Le Formal, F.; Tetreault, N.; Cornuz, M.; Moehl, T.; Gratzel, M.; Sivula, K. *Chem. Sci.* **2011**, *2*, 737.

(15) Zaban, A.; Greenshtein, M.; Bisquert, J. *ChemPhysChem* **2003**, *4*, 859.